of primary ignition''), in *Zababakhinskie Nauchnye Chteniya: Mezhdunar. Konf. 8–12 Sent. 2003, Snezhinsk, Chelyab. obl., Russia. Tezisy* (Zababakhin Scientific Talks: Intern. Conf. 8–12 Sep. 2003, Snezhinsk, Chelyabinsk region, Russia. Theses) (Snezhinsk: Izd. RFYaTs — VNIITF, 2003) p. 106

PACS numbers: 75.30.Sg, **75.80.+q**, 81.30.Kf
DOI: 10.1070/PU2006v049n08ABEH006081

Magnetic shape-memory alloys: phase transitions and functional properties

V D Buchelnikov, A N Vasiliev, V V Koledov, S V Taskaev, V V Khovaylo, V G Shavrov

1. Introduction

The discovery of the effect of giant deformations due to a magnetically induced rearrangement of martensite twins in Heusler alloys Ni_2MnGa [1] attracted significant attention to shape-memory alloys. As a result of intense research in this field, magnetically induced strains as large as 10%, which can be controlled by a magnetic field of about 1 T, have been realized in Ni-Mn-Ga single crystals, and a number of new families of ferromagnets with a shape-memory effect have been revealed [2].

In this report, we review the art and science of theoretical and experimental investigations of phase transitions in ferromagnetic Heusler alloys with the shape-memory effect and of related giant changes in entropy and strain under the effect of an applied magnetic field. Attention is mainly paid to new results concerning the investigations of Ni-Mn-Ga alloys. In particular, we analyze the results of investigations of the specific features of the phase diagram of these alloys and their physical properties in the nanocrystalline state.

2. Magnetic and structural phase transitions

2.1 Phenomenological theories

To describe phase transitions in Ni-Mn-Ga alloys, we first consider the Landau functional [3–8]

$$
\begin{aligned}
F = {} & -Ae_1 + \frac{1}{2}\,A_0 e_1^2 + \frac{1}{2}\,a_1(e_2^2+e_3^2) + De_1(e_2^2+e_3^2) \\
& + \frac{1}{3}\,be_3(e_3^2-3e_2^2) + \frac{1}{4}\,c(e_2^2+e_3^2)^2 + \frac{1}{2}\,A_1|\psi|^2 + \frac{1}{4}\,A_2|\psi|^4 \\
& + \frac{1}{6}\,C_0|\psi|^6 + \frac{1}{6}\,C_1\left[\psi^6 + (\psi^*)^6\right] \\
& + \left(\frac{1}{\sqrt{3}}\,D_1e_1 + \frac{2}{\sqrt{6}}\,D_2e_3 + D_3e_4\right)|\psi|^2 + \frac{1}{2}\,\alpha_1\mathbf{m}^2 + \frac{1}{4}\,\delta_1\mathbf{m}^4 \\
& + K(m_x^2m_y^2 + m_y^2m_z^2 + m_z^2m_x^2) + \frac{1}{\sqrt{3}}\,B_1e_1\mathbf{m}^2 \\
& + B_2\left[\frac{1}{\sqrt{2}}\,e_2(m_x^2-m_y^2) + \frac{1}{\sqrt{6}}\,e_3(3m_z^2-\mathbf{m}^2)\right] \\
& + B_3(e_4m_xm_y + e_5m_ym_z + e_6m_zm_x) \\
& + \left[N_1\mathbf{m}^2 + N_2\left(m_z^2 - \frac{1}{3}\,\mathbf{m}^2\right) + N_3m_xm_y\right]|\psi|^2 + Pe_1\,, \quad (1)
\end{aligned}
$$

where e_i are the linear combinations of the strain tensor components: $e_1 = (e_{xx}+e_{yy}+e_{zz})/\sqrt{3}$, $e_2 = (e_{xx}-e_{yy})/\sqrt{2}$, $e_3 = (2e_{zz}-e_{yy}-e_{xx})/\sqrt{6}$, $e_4 = e_{xy}$, $e_5 = e_{yz}$, $e_6 = e_{zx}$; ψ is the order parameter that describes the modulation of the crystal lattice and is related to the displacement vector $\mathbf{u}$ along the $[\bar{1}10]$ axis as $\mathbf{u}(\mathbf{r}) = |\psi|\mathbf{p}\sin(\mathbf{kr}+\varphi)$, where $\psi = |\psi|\exp(i\varphi)$, $\mathbf{k} = (1/3)[110]$, and $\mathbf{p}$ is the polarization vector; A is a coefficient proportional to the thermal expansion coefficient; $A_0 = (c_{11}+2c_{12})/\sqrt{3}$ is the bulk elasticity modulus; a_1, b, D, and c_1 are linear combinations of elasticity moduli of the second, third, and fourth orders,

$$
a_1 = c_{11} - c_{12}\,, \qquad b = \frac{c_{111} - 3c_{112} + 2c_{123}}{6\sqrt{6}}\,,
$$

$$
D = \frac{c_{111} - c_{123}}{2\sqrt{3}}\,, \qquad c = \frac{c_{1111} + 6c_{1112} - 3c_{1122} - 8c_{1123}}{48}\,;
$$

$\mathbf{m} = \mathbf{M}/M_0$ is the unit magnetization vector; M_0 is the saturation magnetization; B_1 is the constant of volume (exchange) magnetostriction; B_2 and B_3 are the constants of anisotropic (relativistic) magnetostriction; K is the first constant of cubic anisotropy; α_1 and δ_1 are the exchange constants; A_1, A_2, C_0, and C_1 are the coefficients of the expansion of the functional into a series in powers of the modulation order parameter ψ; D_i are the coupling coefficients of the deformation and modulation order parameters; N_i are the coupling constants of the modulation order parameter to the magnetization; and P is the hydrostatic pressure.

The equilibrium states of a cubic ferromagnet can be determined from thermodynamic potential (1) using the standard minimization procedure. The solution of this problem, which can be found both analytically and numerically, has been obtained in several works (see [2] and the references therein).

We note that in $Ni_{2+x}Mn_{1-x}Ga$ alloys, the sign of the first cubic anisotropy constant K depends on the composition [9, 10]. Therefore, the cases where $K > 0$ and $K < 0$ must be considered within a theoretical description of phase transitions (see Refs [66, 67, 91, 200–210] and [211–215] in [2] for $K < 0$ and $K > 0$, respectively).

Investigations of the effect of magnetostriction and modulation of the crystal lattice on the phase transition in Ni-Mn-Ga alloys show that, with the modulation order parameter taken into account, the martensitic transformation is accompanied by either premartensitic or intermartensitic phase transitions [7, 11].

Taking the magnetoelastic interaction into account leads to the appearance of a domain of the existence of combined magnetic and structural (magnetostructural) phase transitions in the phase diagram of $Ni_{2+x}Mn_{1-x}Ga$ alloys [12, 13]. Estimates show that the magnetostructural phase transition in the temperature–composition ($T-x$) phase diagram is realized in a very narrow range of x. Recent experimental studies of the $T-x$ phase diagram of Ni-Mn-Ga alloys in a wider composition range [14] showed that the magnetostructural transition is realized in a rather wide composition interval from $x = 0.18$ to $x = 0.27$ (Fig. 1). In this concentration range, the alloys undergo a transition from a cubic paramagnetic phase into a tetragonal ferromagnetic phase. In this transformation, we can therefore neglect the magnetostriction related to anisotropy and consider only the volume magnetostriction, which is usually large just in the region of a magnetic phase transition. The phase diagram

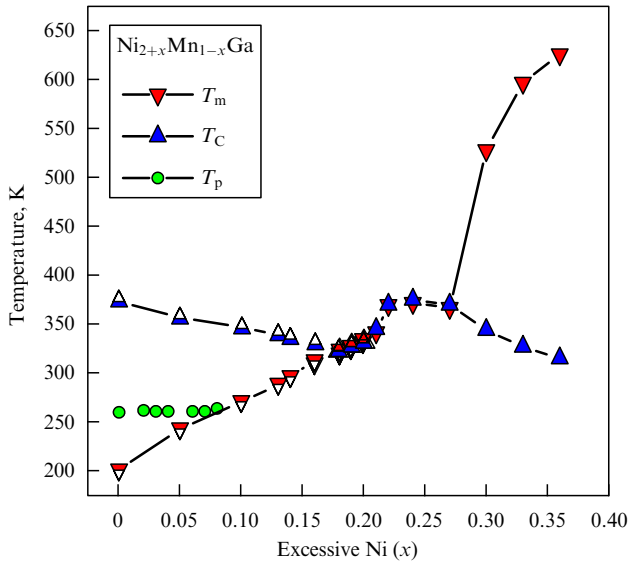

Figure 1. Temperatures of martensitic (T_m), magnetic (T_C), and premartensitic (T_p) phase transitions as functions of excessive Ni in $Ni_{2+x}Mn_{1-x}Ga$ alloys [14–16].

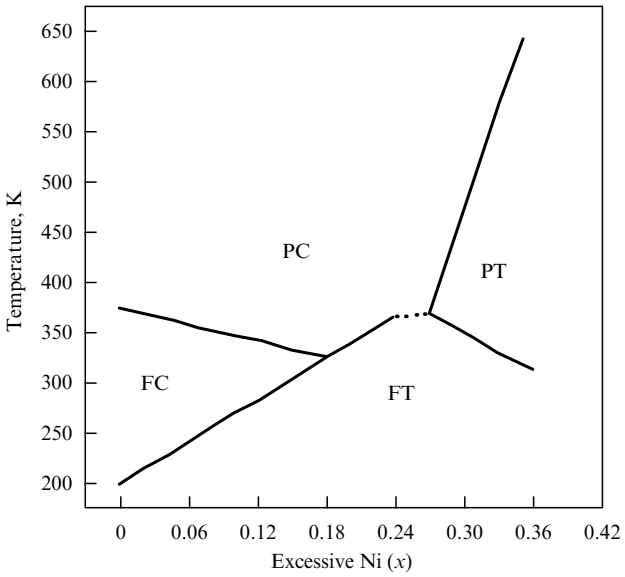

Figure 2. Theoretical phase diagram of $Ni_{2+x}Mn_{1-x}Ga$ alloys in the concentration range $0 < x < 0.36$ with the volume magnetostriction taken into account. Solid straight lines correspond to phase transition lines [8]; PC and PT stand for paramagnetic cubic and tetragonal phases, respectively; FC and FT mean ferromagnetic cubic and tetragonal phases, respectively.

of $Ni_{2+x}Mn_{1-x}Ga$ alloys with volume magnetostriction taken into account was constructed in [8]. To estimate the possibility of the existence of a magnetostructural transition interval, we must know the magnitude of the volume magnetostriction B_1. It was determined in [14, 17] from a comparison of the theoretical jump in the thermal expansion coefficient ($\Delta\varkappa = \varkappa_F - \varkappa_P = B_1\alpha_0/(\sqrt{3}A_0T_C^0\delta)$ [14]) and its experimentally determined value for the stoichiometric Ni_2MnGa alloy. Here, $\varkappa_F$ and $\varkappa_P$ are the respective thermal expansion coefficients in the ferromagnetic and paramagnetic phases; α_0 is the coefficient in the series expansion (in the temperature) of the renormalized (with respect to magnetostriction) exchange constant α_1 near the Curie temperature dependent on the composition x: $T_C(x) = T_C^0 - \gamma x$, where γ is a coefficient determined from experiment; $\alpha_1 = \alpha_0(T - T_C)/T_C^0$, T_C^0 is the Curie temperature for the stoichiometric composition; and δ is the δ_1 constant renormalized with respect to magnetostriction. The magnetostriction magnitude thus determined turned out to be $B_1 = 21 \times 10^9$ erg cm^{-3}. This value of the magnetostriction constant permitted us to theoretically estimate the composition interval of the existence of the magnetostructural phase transition as $\Delta x = x_{fin} - x_{in} \approx 0.08$, which agrees well with experimental data (see Fig. 1).

The theoretical $T-x$ phase diagram with only volume magnetostriction take into account and a linear dependence of the martensitic and magnetic phase transition temperatures on the composition assumed is shown in Fig. 2 by solid lines. It is seen that there is good agreement between theory and experiment. It follows from experimental data that on the line of the magnetostructural phase transition near $x \approx 0.27$, a substantial deviation from the linear dependence is observed; the corresponding segment is shown in Fig. 2 by a dashed line.

2.2 Magnetostructural transition

An analysis of the effect of volume magnetostriction on the phase diagram of $Ni_{2+x}Mn_{1-x}Ga$ alloys performed in [8, 14, 17] shows that it can well explain the existence of a sufficiently large range of compositions where a coupled magnetostructural transition can occur in these alloys.

From the experimental standpoint, this feature of the phase diagram of $Ni_{2+x}Mn_{1-x}Ga$ alloys can be explained as follows. The available experimental data show that the compositional dependence of the martensitic transformation temperature T_m in Ni-Mn-Ga alloys correlates with the concentration of valence electrons e/a; therefore, these alloys can be classified as Hume–Rothery alloys [18]. The martensitic transition occurs as a result of contact of the Fermi surface with the Brillouin zone boundary [19]. Such a model suggests that a change in the number of valence electrons and the modification of the Brillouin zone boundary are the principal factors responsible for the appearance of structural instabilities in these alloys. Neglecting the effects of hybridization and other factors, such as the difference in the electronegativities [20], we can expect a linear variation of T_m with composition caused by changes in the number of valence electrons and chemical pressure, which is indeed observed in some composition intervals in $Ni_{2+x}Mn_{1-x}Ga$ [15], $Ni_{2+x}MnGa_{1-x}$ [21], and $Ni_2Mn_{1+x}Ga_{1-x}$ [22] alloys. However, this scenario is fulfilled when approaching the Curie point, because the volume magnetostriction substantially affects the lattice parameters. In this sense, the peak of the thermal expansion coefficient observed at the Curie point T_C can be regarded as a potential barrier to a further increase in the martensitic transformation temperature T_m, which becomes 'blocked' at the temperature of this peak. A further change in T_m correlates with a change in the Curie temperature T_C; i.e., T_m and T_C are interdependent in some composition interval. To separate these phase transitions, we must reach a concentration e/a that is sufficient to overcome this barrier caused by the volume magnetostriction.

The coincidence of the temperatures of the martensitic and magnetic transitions T_m and T_C is also observed in other ferromagnetic shape-memory alloys, e.g., Co-Ni-X (X = Al,

Ga) [23, 24], Ni-Fe-Ga [25, 26], and Ni-Mn-X (X = In, Sn, Sb) [27, 28]. In Ni-Mn-Ga, the merging of T_m and T_C is observed for various sections of the ternary phase diagram. In the $Ni_{2+x}Mn_{1-x}Ga$ system, T_m and T_C coincide in the alloy of composition $Ni_{2.18}Mn_{0.82}Ga$ [15]. This effect also occurs in $Ni_2Mn_{1+x}Ga_{1-x}$ alloys with extra Mn instead of Ga [22] and in alloys where Ni atoms are partially replaced by Ga atoms [21].

2.3 Phase diagrams of ferromagnetic Heusler alloys with a shape-memory effect

The results of studies of $Ni_{2+x}Mn_{1-x}Ga$ and $Ni_2Mn_{1+x}Ga_{1-x}$ alloys showed their universal tendency to increase T_m and decrease T_C with a deviation of the alloy composition from stoichiometric. The increase in T_m in these alloys can be related to an increase in the electron concentration e/a. Although the first-principle calculations [29] of nonstoichiometric Ni_2MnGa alloys show that the change in the electronic structure caused by deviations of the alloy composition from stoichiometric cannot be described in terms of the 'rigid-band' model, the empirical dependence between the electron concentration and the martensitic transition temperature [18] indicates the applicability of this model. The decrease in T_C that is observed in $Ni_{2+x}Mn_{1-x}Ga$ and $Ni_2Mn_{1+x}Ga_{1-x}$ with increasing x is likely to be due to different factors. In the Ni-Mn-Ga alloys, the magnetic moment, which is equal to $\sim 4\,\mu_B$, is caused by Mn atoms, and hence the T_C decrease in $Ni_{2+x}Mn_{1-x}Ga$ can be explained by the dilution of the magnetic subsystem due to a decrease in the Mn content. For alloys with an excess of Mn atoms (in $Ni_2Mn_{1+x}Ga_{1-x}$), the weakening of exchange interactions can be due to an antiferromagnetic interaction of the excessive Mn atoms [30], although this assumption needs an experimental test. A systematic study of magnetic properties of $Ni_{2+x}Mn_{1-x}Ga$ alloys [31] showed that both the interatomic spacing and the overlap of electron orbitals play an important role in the changes of the exchange parameters upon the structural transformation and that the exchange interactions are stronger in the martensitic state.

The phase diagrams of other ferromagnets with a shape-memory effect have been studied in less detail. The available experimental results indicate a common tendency in the behavior of the structural phase transition upon deviations from the stoichiometric composition: in all ferromagnetic shape-memory Heusler alloys, the temperature of the martensitic transformation increases with increasing the electron concentration e/a [23, 25, 27]. This feature indicates that, evidently, the structural instability in Heusler alloys has a universal origin.

As is known, premartensitic and intermartensitic transitions are observed in Ni-Mn-Ga alloys in addition to the martensitic transformation [2]. The premartensitic transition, which manifests itself in the modulation of the crystal structure of the austenitic phase with the lattice symmetry preserved, is observed for Ni-Mn-Ga compositions close to stoichiometric. The results of some works suggest that either the premartensitic transition or clearly pronounced pretransition phenomena also exist in some compositions of the Ni-Fe-Ga system [32–34]. In other ferromagnets with the shape-memory effect, no premartensitic phase transitions are observed, to the best of our knowledge. Apart from the Ni-Mn-Ga system, the existence of intermartensitic transitions from one crystallographic modification of the martensitic phase into another was also reported for Ni-Fe-Ga [35, 36] and Ni-Mn-X (X = In, Sn) [27] alloys. Because both the premartensitic and, as a rule, martensitic phases are modulated, the formation of superstructural motifs is ascribed to nesting features of the Fermi surface [37, 38].

2.4 Phase transitions in the nanocrystalline state

Physical properties of solids change fundamentally when a nanocrystalline structure is created in them by severe plastic deformation, i.e., by refining crystallites to dimensions of 10–100 nm under high pressure [39]. The authors of Refs [40–42] obtained nanocrystalline ferromagnetic shape-memory alloys of the Ni-Mn-Fe-Ga system and studied the effect of the nanostructure on the martensitic transformation and magnetic ordering and then the effect of subsequent annealings on them. It was shown by electron microscopy that the sample subjected to severe plastic deformation consists of very small-dimension (< 5 nm) crystallites that have no distinct boundaries between them. The subsequent annealing restores the crystallite structure.

Figure 3a displays the temperature dependence of the magnetization of the initial coarse-grained sample. The anomalies at $T_C = 350$ K, $T_m = 290$ K, and $T_I = 230$ K correspond respectively to the Curie temperature and martensitic and intermartensitic transitions. In the nanocrystalline state, the alloy under consideration does not exhibit ferromagnetic properties. The subsequent annealing leads first to restoration of the ferromagnetic ordering and then to restoration of the anomalies related to the structural transition (T_m). However, the intermartensitic transition is not restored (Fig. 3b), which is also confirmed by measurements of electric conductivity.

The disappearance of a long-range order and the suppression of structural phase transitions can arguably be explained by atomic disordering of the alloy in the process of severe plastic deformation and by the effect of the crystallite size on the formation of a magnetically ordered state. A similar situation was revealed in a series of papers [43–45] devoted to the investigation of the effect of the degree of ordering on magnetism and structural transformation of Ni_2MnGa films obtained in a quasiamorphous state by vacuum deposition onto a cooled substrate.

3. Functional properties

3.1 Magnetomechanical effects

If the magnetization of the martensitic phase differs from the magnetization of the austenitic phase, the application of a magnetic field leads to a shift in the temperature of the structural transformation, i.e., to a stabilization of the phase with a larger magnetization [46]. This effect can be used to obtain giant magnetostrains in the temperature range of the martensitic transformation. Investigations in Refs [47–49] were aimed at creating functional materials based on $Ni_{2+x+y}Mn_{1-x}Ga_{1-y}$ alloys in which a giant magnetostrain is reached due to the shift in the martensitic transition temperature. A magnetic-field-controlled reversible shift in the temperature of the martensitic transformation in $Ni_{2+x}Mn_{1-x}Ga$ ($x = 0.16-0.19$) was observed in [48]. The shape-memory effect induced by a magnetic field and the related giant magnetostrains were investigated in polycrystalline samples of $Ni_{2+x-y}Mn_{1-x}Fe_yGa$ alloys [47]. Additions of iron were found to improve the mechanical properties of the $Ni_{2+x}Mn_{1-x}Ga$ alloys. To obtain a two-way shape-memory

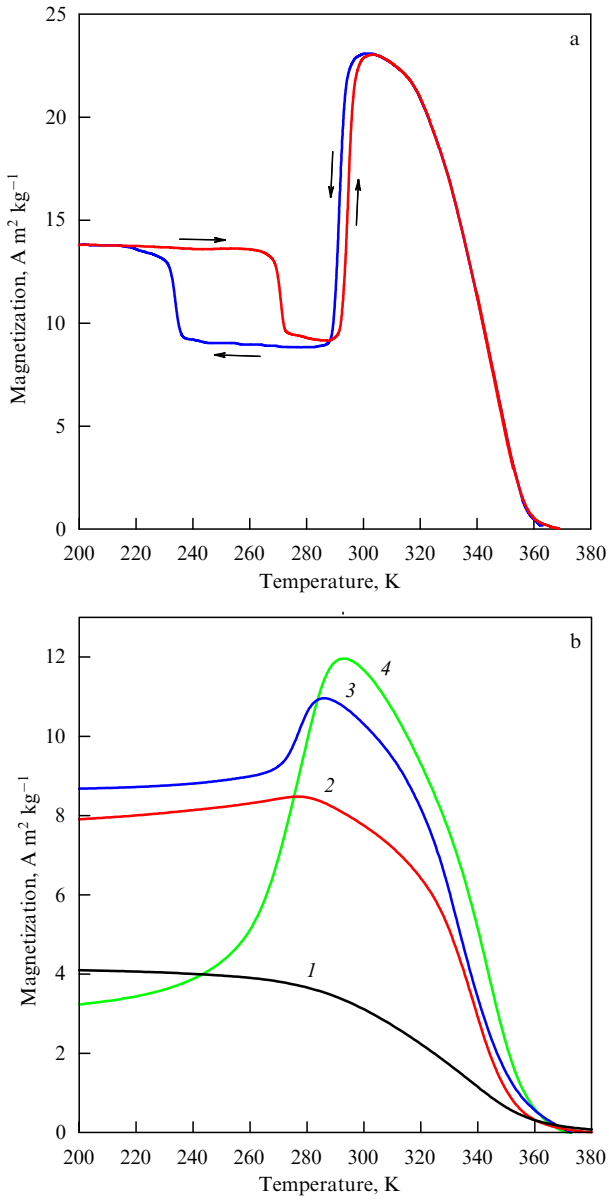

Figure 3. (a) Temperature dependences of the magnetization of a coarse-grained $Ni_{2.14}Mn_{0.81}Fe_{0.05}Ga$ alloy in the external magnetic field $H = 1$ T. (b) Temperature dependences of the magnetization of a nanocrystalline sample of the $Ni_{2.14}Mn_{0.81}Fe_{0.05}Ga$ alloy in the external magnetic field $H = 1$ T after annealing at various temperatures: (*1*) 623, (*2*) 673, (*3*) 773, and (*4*) 1073 K [41].

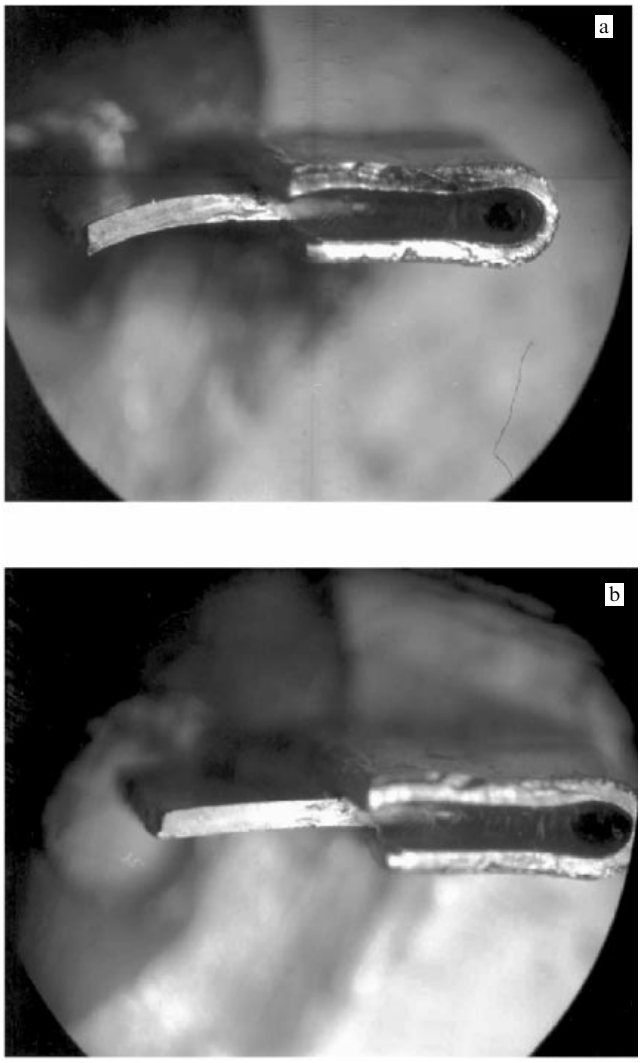

Figure 4. Photographs of a sample used in the experiments on the magnetically controlled shape-memory effect: (a) the magnetic field is switched on and (b) switched off [47].

effect, samples in the form of plates were 'trained' by thermocycling under a load. The training led to an increase in the limiting bending deformation from 2% for the untrained sample to 4.5% in samples subjected to multiple thermocycling. A shape-memory effect caused by the shift of the martensitic-transformation temperature by a magnetic field was observed in a trained platelet of the $Ni_{2.15}Mn_{0.81}Fe_{0.04}Ga$ alloy with $T_m \sim 313$ K. The experiment was conducted as follows. A plate, which was bent in the martensitic state, was placed at room temperature into the magnetic field $H = 10$ T. Then, the plate was heated in a field to $T = 315$ K and held at this temperature. Under these conditions, the bending deformation was $\sim 3\%$. After the magnetic field was switched off, the plate passed into the austenitic state and became completely unbent (Fig. 4). Thus, the bending deformation $\Delta e = 3\%$ was induced by the magnetic field $H = 10$ T.

The next step in the way of increasing the efficiency of controlling the dimensions and shape of the sample due to the shift of the martensitic transformation temperature was done in [50], where it was shown that with Ni substituted by Co in the Ni(Co)MnIn alloy, the transition of austenite into martensite is accompanied by the transition from the ferromagnetic state with a large saturation magnetization into a supposedly antiferromagnetic state with a zero spontaneous magnetization. Because the extent of the magnetic field effect on the structural transition temperature T_m is determined by the difference in the magnetizations of the high-temperature and low-temperature phases, the application of a magnetic field of 7 T decreased T_m by ~ 30 K. Because the temperature hysteresis of the martensitic transformation in this alloy is ~ 8 K, the reversible structural transition can be induced by a magnetic field that does not exceed 3 T. The experiments show that to obtain a 3% strain caused by the shift of the martensitic transformation temperature in a single-crystal sample, it suffices to apply a magnetic field equal to ~ 4 T.

Another mechanism of obtaining giant magnetostrains is the reorientation of martensitic variants by a magnetic field. This mechanism was suggested in [51] and realized for the first time in [1], where a strain of 0.2% induced by a magnetic field of 0.8 T in a single crystal of the Ni_2MnGa Heusler alloy with the martensitic transformation temperature $T_m \sim 276$ K was reported. Later, 6% strains in the martensitic phase of single-crystals with a five-layer modulation were obtained [52]. Also reported was the occurrence of an irreversible 9% deformation in a single crystal with a seven-layer modulation [53]. An analysis of the dynamics of motion of martensitic variants under the effect of an ac magnetic field shows [54] that the response of the system to an external action can be observed up to the frequencies about 2 kHz.

From the standpoint of practical applications, the above-considered methods for obtaining giant magnetostrains in ferromagnets with a shape-memory effect have both advantages and drawbacks. For example, the advantages of producing magnetostrains due to the shift in the martensitic-transition temperature are the possibility of using inexpensive polycrystals, the universality of the deformation mode (linear deformations, bending, twisting), and the possibility of controlling deformations in actuators on a micron and submicron level. The shortcomings of this method are a relatively narrow range of working temperatures and the necessity in strong magnetic fields (about 10 T). We note, however, that recently observed results [50] give confidence that these drawbacks can be overcome.

3.2 The giant magnetocaloric effect in the magnetostructural transition

The problem of the investigation of the magnetocaloric effect in materials with a magnetostructural transition has been considered in numerous works. The greatest attention is paid to the alloys based on Gd(SiGe), (MnFe)(PAs), and La-Fe-Si [55]. The giant magnetocaloric effect observed in these alloys is due to the magnetostructural transition. It occurs at a temperature that is determined by the composition and can be close to room temperature. Such a possibility opens prospects for creating refrigerators working at room temperature for wide applications in industry and in private life. Of special interest are Heusler alloys, because they are ecological and do not contain poisonous or expensive rare-earth metals.

In Ni-Mn-Ga alloys with a coupled magnetostructural transition, the magnetocaloric effect has been studied in most detail in the case of the alloy of composition $Ni_{2.19}Mn_{0.81}Ga$ [56–59]. For this alloy, direct measurements of the adiabatic variation of the temperature upon the application of a magnetic field have been performed [58, 59], apart from the determination of the magnetocaloric effect from the results of the most common method — measurements of isothermal magnetization curves. The experimental $\Delta S(T)$ dependences determined from direct measurements are shown in Fig. 5. The curves have two sharp peaks at the temperatures 338 K and 344 K. In a magnetic field of 2.6 T, the greatest change in the entropy is 9 J kg^{-1} K^{-1} when the field is switched on at 338 K and 11 J kg^{-1} K^{-1} when the field is switched off at 344 K. The values of the magnetocaloric effect obtained (10 J kg^{-1} K^{-1}) are close to the best values observed at room temperature for other known materials with the giant magnetocaloric effect [55]. The results of calculations based on the theory described in [57, 60, 61] give curves that agree well with the experimental results (see Fig. 5).

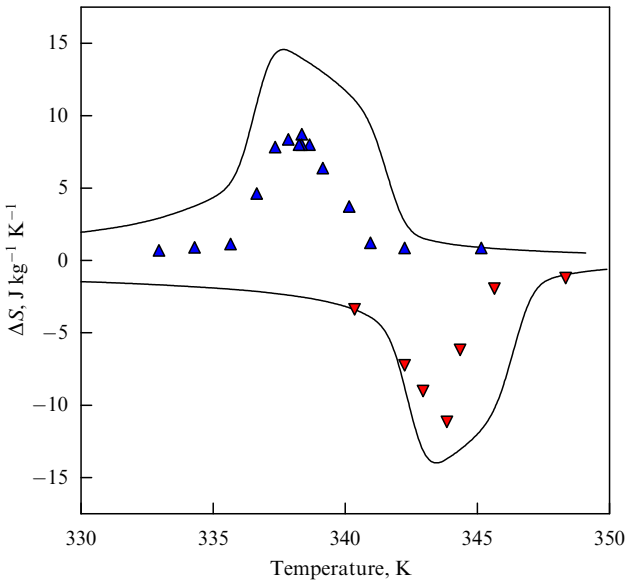

Figure 5. Direct measurements of the magnetocaloric effect in the $Ni_{2.19}Mn_{0.81}Ga$ alloy in the field 2.6 T. Symbols, experimental data points; solid curves, theory [59].

The giant magnetocaloric effect was observed not only in Ni-Mn-Ga alloys but also in Ni-Mn-Sn alloys [62]. We note that in the latter, the difference ΔS is positive. This is because the structural transition occurs from the austenitic ferromagnetic phase to the martensitic phase with a dominating antiferromagnetic exchange.

4. Applied capabilities of functional materials based on ferromagnetic alloys with the shape-memory effect

The discovery of the effect of giant strains caused by a rearrangement of martensitic variants in Ni-Mn-Ga single crystals under the action of a magnetic field [1] has attracted great attention to this problem. Only a few years later, commercial samples of actuators based on this material appeared on the market [63]. The results of ten years of work on the improvement of the extremely attainable parameters of the Ni-Mn-Ga alloys are as follows: the maximum limiting strains (compression – tension) up to 9.5% [53]; the recovery stress 2 MPa [52]; and the minimum response time 150 μs [54]. Commercial actuators produced by Adaptamat, Inc. (patents [64, 65]) ensure the following characteristics: the displacement of the actuating element up to 5 mm; frequency up to 1000 Hz; and the force up to 1000 N [63]. This technology is expensive and complex because of the necessity of using perfect single crystals; however, we cannot deny its potential, e.g., in the technology of hydroacoustic transducers.

It is obvious that the applied potential of the new materials is by no means exhausted by this application. Of great interest is the possibility of controlling the shape and dimensions of ferromagnets having the shape-memory effect by using a magnetically induced martensitic transformation [47, 48]. In the case of this mechanism, the actuating element (preliminarily trained for a two-way shape-memory effect) can change its shape under the effect of a magnetic field at a constant temperature in an arbitrary manner, i.e., can be bent, twisted, stretched, etc. These properties can find

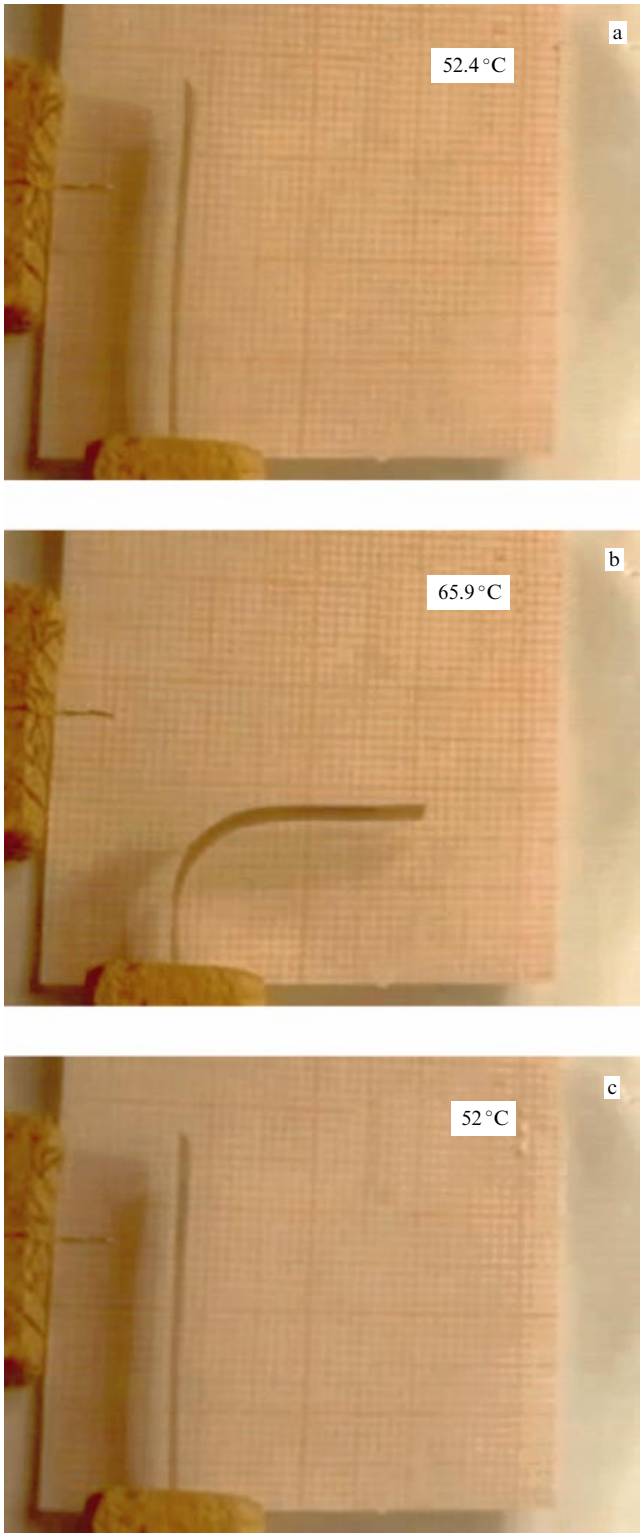

Figure 6. Variation in the shape of a bimetallic composite based on a shape-memory alloy: (a) in the low-temperature phase; (b) upon heating to above the martensitic transformation temperature; and (c) upon cooling to the low-temperature phase.

application in electronics, micro- and nanomechanics, and medicine.

The active elements of ferromagnets with the shape-memory effect have the property of changing their magnetic susceptibility upon the martensitic transformation and, consequently, upon pseudoplastic deformation. In devices similar to that described in [66], the magnetic state of the actuator itself serves as both the cause and the indicator of its mechanical state. Consequently, such a device combines the functional opportunities of a sensor and an actuator.

Recently, a new principle for creating reversible bending strains was suggested based on the use of layered composites consisting of ferromagnetic or nonferromagnetic materials with a shape-memory effect. This principle is analogous to the action of a bimetallic or a bimagnetostrictive plate, but the limiting reversible bending strains can in principle be greater by 1 – 3 orders of magnitude. Figure 6 shows the prototype of a composite whose bending is controlled by heating.

Acknowledgments. This work was supported in part by the Russian Foundation for Basic Research (project nos 04-02-81058-Bel, 05-02-19935-YaF, 05-0850341, 06-02-16266, and 06-02-16984); grants from the President of the Russian Federation (nos NSh-8269.2006.2, MK-5658.2006.2); a grant from the Ministry of Education of the Russian Federation and CRDF Y2-P-05-19; and a grant from the Ministry of Economic Development of the Chelyabinsk region.

References

1. Ullakko K et al. *Appl. Phys. Lett.* **69** 1966 (1996)
2. Vasil'ev A N et al. *Usp. Fiz. Nauk* **173** 577 (2003) [*Phys. Usp.* **46** 559 (2003)]
3. Fradkin M A *Phys. Rev. B* **50** 16326 (1994)
4. Izyumov Yu A, Syromyatnikov V N *Fazovye Perekhody i Simmetriya Kristallov* (Phase Transitions and Crystal Symmetry) (Moscow: Nauka, 1984) [Translated into English (Dordrecht: Kluwer Acad. Publ., 1990)]
5. Krumhansl J A, Gooding R J *Phys. Rev. B* **39** 3047 (1989)
6. Gooding R J, Krumhansl J A *Phys. Rev. B* **38** 1695 (1988)
7. Buchel'nikov V D et al. *Zh. Eksp. Teor. Fiz.* **119** 1166 (2001) [*JETP* **92** 1010 (2001)]
8. Buchelnikov V D et al. *J. Magn. Magn. Mater.* **290 – 291** 854 (2005)
9. Tickle R, James R D *J. Magn. Magn. Mater.* **195** 627 (1999)
10. Shanina B D et al. *J. Magn. Magn. Mater.* **237** 309 (2001)
11. Buchelnikov V et al. *Int. J. Appl. Electromagn. Mech.* **12** 19 (2000)
12. Buchel'nikov V D et al. *Zh. Eksp. Teor. Fiz.* **119** 1176 (2001) [*JETP* **92** 1019 (2001)]
13. Zayak A T, Buchelnikov V D, Entel P *Phase Trans.* **75** 243 (2002)
14. Khovaylo V V et al. *Phys. Rev. B* **72** 224408 (2005)
15. Vasil'ev A N et al. *Phys. Rev. B* **59** 1113 (1999)
16. Khovailo V V et al. *J. Phys.: Condens. Matter* **13** 9655 (2001)
17. Buchelnikov V D, Khovailo V V, Takagi T *J. Magn. Magn. Mater.* **300** e459 (2006)
18. Chernenko V A *Scripta Mater.* **40** 523 (1999)
19. Webster P J et al. *Philos. Mag. B* **49** 295 (1984)
20. Watson R E, Weinert M, in *Solid State Physics* Vol. 56 (Eds H Ehrenreich, F Spaepen) (New York: Academic Press, 2001) p. 1
21. Lanska N et al. *J. Appl. Phys.* **95** 8074 (2004)
22. Jiang C et al. *Acta Mater.* **52** 2779 (2004)
23. Oikawa K et al. *Mater. Trans.* **42** 2472 (2001)
24. Oikawa K et al. *Appl. Phys. Lett.* **79** 3290 (2001)
25. Oikawa K et al. *Appl. Phys. Lett.* **81** 5201 (2002)
26. Oikawa K et al. *Mater. Trans.* **43** 2360 (2002)
27. Sutou Y et al. *Appl. Phys. Lett.* **85** 4358 (2004)
28. Krenke T et al. *Phys. Rev. B* **72** 014412 (2005)
29. MacLaren J M *J. Appl. Phys.* **91** 7801 (2002)
30. Enkovaara J et al. *Phys. Rev. B* **67** 212405 (2003)
31. Khovailo V V et al. *Phys. Rev. B* **70** 174413 (2004)
32. Li J Q et al. *Solid State Commun.* **126** 323 (2003)
33. Murakami Y et al. *Appl. Phys. Lett.* **82** 3695 (2003)
34. Oikawa K et al. *J. Magn. Magn. Mater.* **272 – 276** 2043 (2004)
35. Sutou Y et al. *Appl. Phys. Lett.* **84** 1275 (2004)
36. Zheng H X et al. *J. Alloys Comp.* **385** 144 (2004)
37. Zheludev A et al. *Phys. Rev. B* **54** 15045 (1996)

38. Velikokhatnyi O I, Naumov I I *Fiz. Tverd. Tela* **41** 684 (1999) [*Phys. Solid State* **41** 617 (1999)]
39. Gusev A I, Rempel' A A *Nanokristallicheskie Materialy* (Nanocrystalline Materials) (Moscow: Fizmatlit, 2000); see also *Nanocrystalline Materials* (Cambridge: Cambridge Intern. Sci. Publ., 2004)
40. Imashev R N et al. *Dokl. Ross. Akad. Nauk* **400** 333 (2005) [*Dokl. Phys.* **50** 28 (2005)]
41. Imashev R N et al. *J. Phys.*: *Condens. Matter* **17** 2129 (2005)
42. Imashev R N et al. *Fiz. Tverd. Tela* **47** 536 (2005) [*Phys. Solid State* **47** 556 (2005)]
43. Sharipov I Z, Mulyukov R R, Mulyukov Kh Ya *Fiz. Met. Metalloved.* **95** (1) 47 (2003) [*Phys. Met. Metallogr.* **95** 42 (2003)]
44. Kim K W et al. *J. Magn. Magn. Mater.* **272 – 276** 1176 (2004)
45. Kim K W et al. *J. Korean Phys. Soc.* **45** 28 (2004)
46. Krivoglaz M A, Sadovskii V D *Fiz. Met. Metalloved.* **18** 502 (1964)
47. Cherechukin A A et al. *Phys. Lett. A* **291** 175 (2001)
48. Dikshtein I E et al. *Pis'ma Zh. Eksp. Teor. Fiz.* **72** 536 (2000) [*JETP Lett.* **72** 373 (2000)]
49. Takagi T et al. *Int. J. Appl. Electromagn. Mech.* **16** 173 (2002)
50. Kainuma R et al. *Nature* **439** 957 (2006)
51. Ullakko K *J. Mater. Eng. Perform.* **5** 405 (1996)
52. Murray S J et al. *Appl. Phys. Lett.* **77** 886 (2000)
53. Sozinov A et al. *Appl. Phys. Lett.* **80** 1746 (2002)
54. Marioni M A, O'Handley R C, Allen S M *Appl. Phys. Lett.* **83** 3966 (2003)
55. Gschneidner K A (Jr), Pecharsky V K, Tsokol A O *Rep. Prog. Phys.* **68** 1479 (2005)
56. Pareti L et al. *Eur. Phys. J. B* **32** 303 (2003)
57. Aliev A et al. *J. Magn. Magn. Mater.* **272 – 276** 2040 (2004)
58. Aliev A M et al., in *Proc. of the First IIR Intern. Conf. on Magnetic Refrigeration at Room Temperature, Montreux, Switzerland, 27 – 30 September 2005*, p. 135
59. Buchelnikov V D et al. *Int. J. Appl. Electromagn. Mech.* (in press)
60. Buchelnikov V D, Bosko S I *J. Magn. Magn. Mater.* **258 – 259** 497 (2003)
61. Bosko S I, Buchelnikov V D, Takagi T *J. Magn. Magn. Mater.* **272 – 276** 2102 (2004)
62. Krenke T et al. *Nature Mater.* **4** 450 (2005)
63. AdaptaMat, http://www.adaptamat.com/
64. O'Handley R C, Ullakko K M, US Patent No. 5958154 (September 28, 1999)
65. Ullakko K M, US Patent No. 6157101 (December 5, 2000)
66. Kohl M et al. *Sensors Actuators A* **114** 445 (2004)